An energetic approach in thermomechanical fatigue for silicium molybden cast iron

E. Charkaluk, Andreï Constantinescu

An energetic approach in thermomechanical fatigue for silicon molybdenum cast iron

E. Charkaluk[1] and A. Constantinescu[2]
[1]P.S.A. Peugeot-Citroën, Direction de la Recherche et de l'Innovation, Chemin de la Malmaison, 91570 Bievres, France
[2]L.M.S, Laboratoire de Mécanique des Solides (CNRS UMR 7649), Ecole Polytechnique, 91128 Palaiseau, France

The purpose of this paper is to define a low cycle fatigue criterion in order to predict the failure of engineering structures. The major problem in defining a predictive fatigue criterion is that it should be applicable for structures submitted to complex multiaxial thermo-mechanical loadings but should be identifiable from simple experiments on specimens. After a short critical review of the principal criteria used in low cycle fatigue it will be shown that the dissipated energy per cycle permits a correlation of isothermal and anisothermal results obtained on silicon molybdenum cast iron in the case of specimens and also on structures.

Keywords: thermomechanical fatigue, silicon molybdenum, cast iron

INTRODUCTION

The prediction of fatigue and failure of structures submitted to thermomechanical loadings is one of the major problems in mechanical engineering and has been the subject of major efforts in the last few decades. The main applications concern the nuclear and the aeronautical industries, and many results are essentially related to safety and lifetime predictions on simplified structures (see for example [1]). However, when mechanical behaviour of real structures submitted to non isothermal multiaxial loading is computed, methods do not integrate to a lifetime prediction [2]. But in a design context one should be able to estimate by computation the response of any complex structure.

There are essentially three major difficulties in attaining this objective : the constitutive law which must be validated in a wide range of temperatures, its efficient implementation in a finite element standard code and the fatigue criterion itself. To be compatible with an industrial structural computation, the constitutive law should permit computer simulations in a relatively small calculation time of elastoviscoplastic structures subjected to complex thermomechanical loadings and the fatigue criterion should predict both isothermal and anisothermal LCF failure in a large range of temperatures and multiaxial loadings. Therefore we should use a simple robust criterion at a global macroscopical level to predict low cycle thermomechanical fatigue failure structures.

This complete approach has recently been illustrated [3] for cast iron exhaust manifolds in an industrial context. As a continuation of that paper, we present here a detailed discussion on the determination of a robust fatigue criterion in a thermomechanical context. After an interpretation of the tests results using classical fatigue criteria, such as Manson-Coffin and Ostergren, it is shown that the dissipated energy per cycle can be considered as a good damage indicator.

β = Manson-Coffin and Ostergren relations exponent
E = Young modulus
$\Delta\epsilon$ = total mechanical strain range
$\Delta\epsilon_p$ = plastic strain range
k = Ostergren relation frequency exponent
N_{sat} = number of cycles to saturation
N_{tan} = number of cycles to tangent point
N_f = number of cycles to failure
ν = frequency
σ_{max} = maximum stress of a cycle
σ_T = maximum tensile stress of a cycle
Δw = dissipated energy density
Δw_{sat} = experimental dissipated energy density at saturation
W_{sat} = cumulated energy to saturation
W_{tan} = cumulated energy to tangent point
W_f = cumulated energy to fracture

The energetic approach has been appraised beginning with the pioneering paper of Feltner and Morrow [4] who asserted that : "…to start with a specimen in one piece and then after the application of a finite number of load cycles find it to be in two pieces, requires a conversion of energy. The energy necessary to cause fracture is collected in small amounts during the course of the cyclic loading and is observable in terms of strain hysteresis". This approach has been justified by experiments. For example, Luong and Dang Van [5] have shown using infrared thermography measurements, that the rate of energy dissipation can be correlated with the fatigue limit of the material and that it can be correlated with classical damage indicators such as plastic strain.

The energetic approach has been heavily criticized as the global dissipated energy per cycle cannot yet be split into dissipated heat and damage accumulation in a convincing manner. Being conscious of this drawback, we shall show in that a precise estimate of the dissipated energy can be conducted as a first approximation of a fatigue criterion unifying LCF and TMF experiments. For structures and loads where it is impossible to obtain closed form solutions, the dissipated energy per cycle in TMF experiments will be obtained from numerical computations. Our results show that the method predicts the lifetimes as well as the damage area (macroscopic cracks).

TESTS AND SPECIMENS

The silicon molybdenum cast iron

The studied material is a silicon molybdenum spheroidal graphite cast iron (SiMo SG cast iron with a composition presented in Table 1) employed in the automotive industry for the production of exhaust manifolds which are subject to temperatures ranging between –20°C and 800°C with heating rates of 10–20°C/s.

The metallographic structure of this material exhibits a ferritic matrix with pearlitic zones especially around grain boundaries and graphite nodules homogeneously dispatched in the matrix (see Figure 1). At high temperatures, pearlitic zones grow around grain boundaries with molybdenum precipitates (see Figure 2).

In isothermal tension–compression tests, the material displays mainly kinematic hardening with stable strain–stress loops being obtained after 20 cycles. Its cyclic behaviour can be considered to be saturated after a very short time, as discussed later in detail.

Low cycle fatigue tests (LCF)

Fully reversed isothermal low cycle fatigue tests ($R_\epsilon = -1$) were carried out in a temperature range of 200–700°C. The specimens have a gauge section of 7 × 20 millimeters (diameter × length). The conditions for each temperature and the number of tests for each conditions are given in Table 2.

Thermal fatigue tests (TMF)

The thermal fatigue tests were conducted on a specific test machine. The specimen was clamped between two cantilever beams and heated by the Joule effect, applying a continuous current at its ends. The temperature was controlled by a spot welded thermocouple in the middle of the specimen. A precise scheme of the machine and the measurement points are presented in Figure 3.

The specimen had a central useful part of dimensions: 12 × 40 mm (diameter × length). The temperature distribution in the specimen varies between 40 and 700°C in the middle and within 40 and 200°C in the ends. The temperature in the ends has been maintained low by continuous water circulation in the hollow heads. In each

Table 1 SiMo SG cast iron composition

Element	C	Si	Mo	Mg	Ni
Weight	3.47	3.86	0.63	0.22	0.56

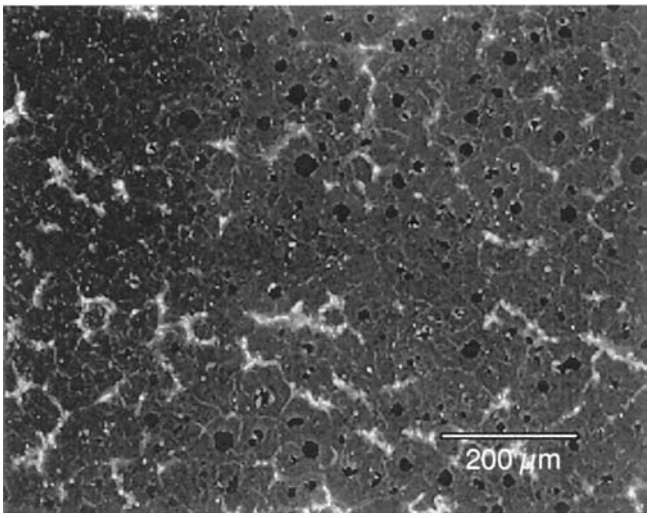

Figure 1 Metallographic structure of the SiMo SG cast iron (ferritic matrix, pearlitic area, carbon nodules) at room temperature

Table 2 Experimental conditions for LCF tests and number of tests for each condition

		Strain range		
Temperature (°C)	Strain rate (s^{-1})	±0.25%	±0.5%	±1%
200	10^{-3}	1	2	2
350	10^{-3}	2	3	1
400	10^{-3}	3	2	
600	10^{-3}	4	3	2
700	10^{-3}	3	2	2

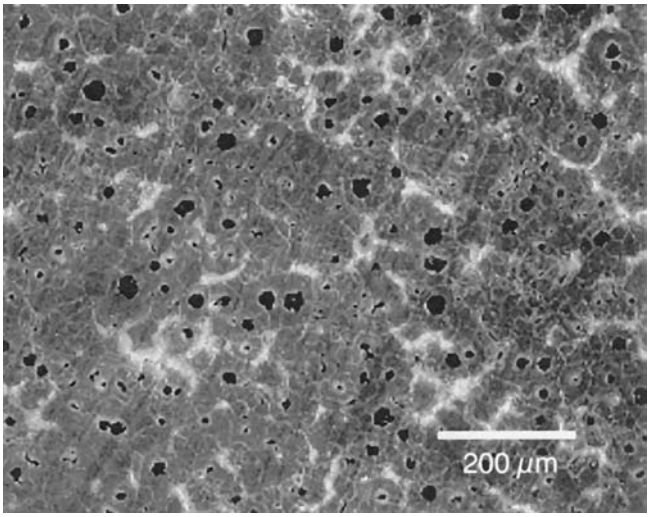

Figure 2 Microsctructure of SiMo cast-iron at 700°C with pearlitic zone at grain boundaries. At room temperature lamellar pearlite became globular.

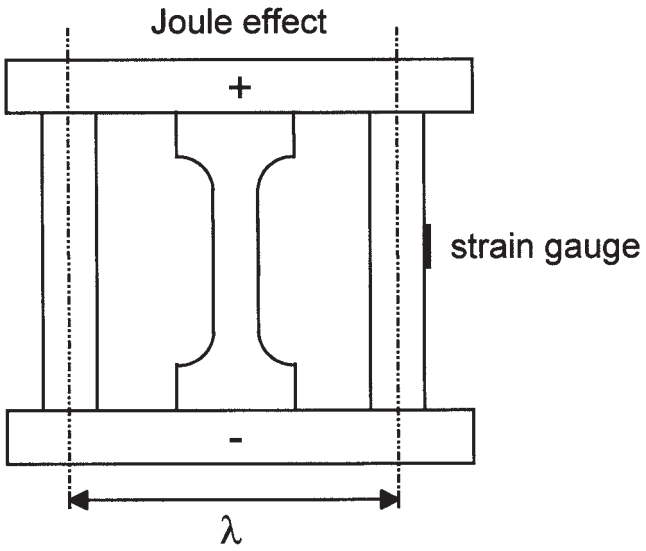

Figure 3 Thermal fatigue tests. An electric current is applied between both extremities of the specimen which is heated by Joule effect.

section, the temperature distribution can be considered constant as long as no major crack appears. Thermal FEM computations showed less than 15°C of radial difference between the center and the surface at the maximum 700°C level.

At the maximum temperature, during the dwell time, the on-off control of the temperature regulation induces temperature variations of ±15°C. FEM analysis has shown that only 5% of the strain variations on the total cumulated strain was due to the dwell time. Therefore these variations will be neglected in the following.

The maximum stress in the specimen is partly related to the axial rigidity of the machine, *i.e.* the sum of the axial rigidity of the pillars and the bending rigidity of the cantilever beams. This rigidity depends on the distance between the two pillars and has been considered as a test parameter (see Table 3). The machine acts as a spring clamped in parallel with the specimen at its ends. Therefore the axial stress in the specimen can be estimated precisely by a strain gauge on the pillars. As an example, axial stresses were of ≈30 MPa in the dwell period at maximum temperature 700°C and of ≈200–400 MPa at room temperature, depending on the machine rigidity.

RESULTS

Microscopic observations of fracture surfaces

As an introduction to the fatigue results some macroscopic observations on fractured specimens for LCF and thermal fatigue tests will be presented and compared with similar aspects observed on steels [6,7].

Table 3 Experimental conditions for thermal fatigue tests on cast-iron corresponding to the machine in Figure 3

temperature range (°C)	clamp rigidity (N/mm)	dwell time (s)	heating rate (°C s^{-1})
40–700	227,000	60	20
40–700	227,000	900	20
40–700	183,000	60	20
40–700	183,000	900	20

A summary of these observations is that LCF test conditions produce *transgranular fatigue crack* growth with a final ductile fracture (see Figure 4) and that TMF tests produce *intergranular fatigue crack* growth with a final ductile fracture (see Figure 5). The inspected fractographic surfaces correspond to 700°C for the LCF tests and to a 1 minute dwell time for the TMF tests.

For LCF tests, the frequency was 3–12 cycles per minute (cpm) corresponding to strain rates of ≈10^{-3} s^{-1} and strain ranges ≈±0.25–±1%.

For TMF tests, the frequency range was 0.06–0.3 cpm and corresponding to thermal strain rates ≈10^{-4} s^{-1}. It is important to notice that the frequency is mainly determined by the dwell time, as the total cycle is approximately divided into 30 seconds of heating, 2 minutes of cooling and 1–15 minutes of dwell time.

It is now obvious that the transgranular and intergranular fatigue crack growth for LCF and TMF tests respectively can also be correlated with the notion of frequency [6,7]. Low frequency TMF tests lead to an intergranular fatigue crack growth characteristic of creep damage whereas high frequency LCF tests lead to transgranular fatigue crack growth. A complete conclusion could only be drawn after performing LCF tests at the same frequency.

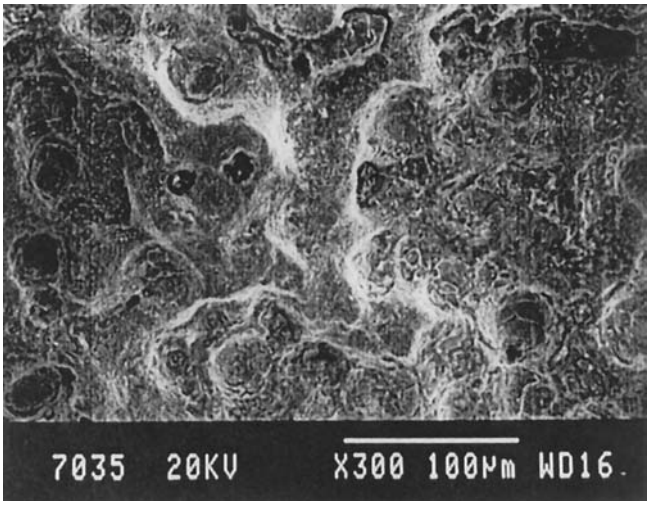

Figure 4 Transgranular fracture surface of a low cycle fatigue specimen tested at 700°C with a strain rate of 10^{-3} s^{-1}.

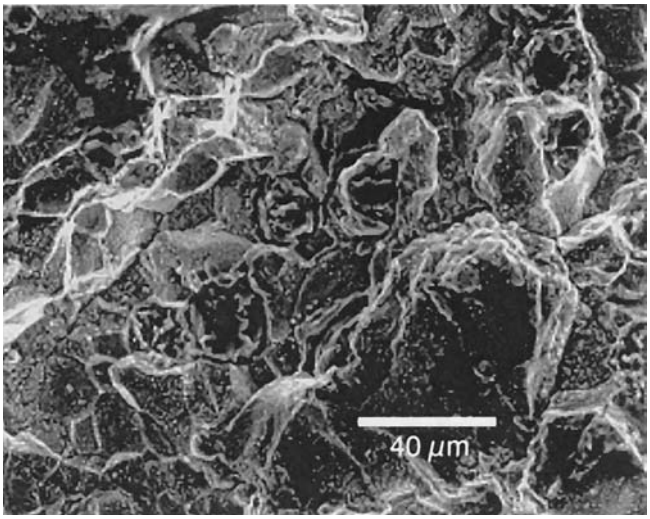

Figure 5 Intergranular fracture surface of a thermal fatigue specimen tested between 40 and 700°C with a mean strain rate of 10^{-4} s^{-1}.

Similar results have been reported on steels by Solomon *et al.* [6] (for A286 steel) and Gell *et al.* [7] (for A304 steel). They reported an intergranular fracture surface at low frequencies (< 0.1 cpm in their case), and a transgranular fracture surface at high frequencies (> 5 cpm). In both cases, the frequencies on cast iron are of the same order as that for steels. More than that, TMF tests show that a dwell time with a tensile stress increased the chances for intergranular failure which was also one of the conclusions in [7].

The observation of fracture surfaces shows that apparently two microscopic mechanisms are driving the failure in different groups of testing conditions. However, in the sequel, we shall focus on the search for a unique global macroscopic quantity characterizing fatigue damage. Therefore the test results will be interpreted from the point of view of classical fatigue criteria, pointing out the difficulties due to the anisothermal and multiaxial context.

Plastic strain range influence

As a first approximation let us interpret the results using the classical Manson-Coffin fatigue criterion [8,9], based on the cumulated plastic strain:

$$\Delta\epsilon_p.N_f^{\beta} = c \qquad (1)$$

where $\Delta\epsilon_p$ is the plastic strain range, N_f is the number of cycles to failure and β and c are material constants. The LCF tests results are reported in Figure 6 and Table 4.

For 200, 600 and 700°C the results can be placed in a scattered band with a factor of ±2 on the number of cycles to failure corresponding to the standard deviation.

The lifetime decreased by a significant factor of 10 between 350 and 400°C. This phenomenon might be explained by dynamic strain aging of cast iron at this temperatures already reported for static loadings by Bastid [10]. To our knowledge, no similar observations have been reported for cast iron for cyclic loading. Further experiments and microscopic observations should be therefore carried out to explain this phenomenon.

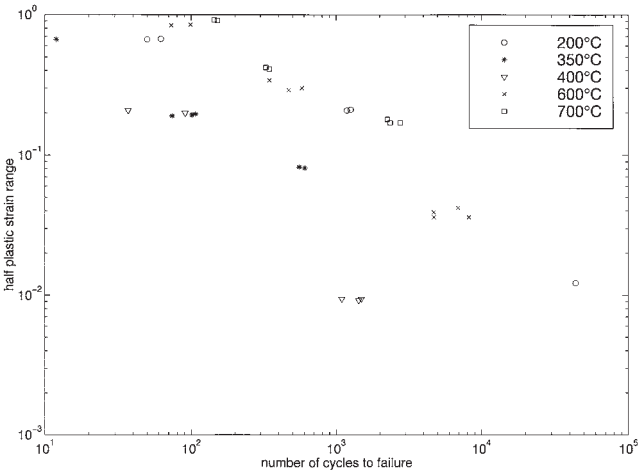

Figure 6 Manson–Coffin results obtained at different temperatures with the SiMo SG cast iron with the test conditions corresponding to Table 2.

Table 4 Exponent of the Manson–Coffin law at different temperatures

Temperature	200°C	350°C	400°C	600°C	700°C
β	0.58	0.53		0.74	0.56

As a first conclusion, we can state that the cumulated plastic strain for cast iron experiments has not been influenced by temperature, except for the important drop in lifetime at 350 and 400°C due to the brittleness. These results are in opposition with the observations made on different steels. A significant influence of temperature has been reported by Coffin [11] on five different steels (A409, A304, A316, A348, A286) and Taira [12] on a 0.16% carbon steel.

The results in [11] show that if the maximum temperature of the cycle T_{max} is smaller than 500°C, damage is controlled by dislocation gliding and the value of the exponent β is close to 0.5 whereas if T_{max} is greater than 500°C, damage is controlled by diffusion phenomena inducing creep and β is close to 1.

Coffin also notices [11] the convergence of the fatigue curves for “very low” cycle fatigue tests (less than 100 cycles). This was not observed for cast iron and probably more tests are needed before drawing a definite conclusion on this item.

In the case of TMF tests the amplitude of plastic strain, $\Delta\epsilon_p$, lacks a precise mechanical interpretation. On one hand the specimen is subject to a temperature gradient and therefore the value of $\Delta\epsilon_p$ depends of the spatial point where the measurement takes place. On the other hand the load cycle is anisothermal, the yield limit is temperature dependent and a strain amplitude would encompass different temperatures with different yield limits and damage influences.

Mean stress influence

In order to refine the previous approach including the effect of a mean stress in LCF tests, Smith *et al.* [13], Jaske [14] and Ostergren [16] included stress in the damage indicator of the lifetime prediction. This change should also take into account the influence of the strain dwells as shown in [15].

With (1) as the lifetime prediction equation, Smith-Topper-Watson (STW) proposed:

$$\sqrt{\sigma_{max}}.\Delta\epsilon.E \qquad (2)$$

as a damage indicator. A similar indicator:

$$\frac{\Delta\epsilon}{2}.\sigma_{max} \qquad (3)$$

was introduced by Jaske[14]. In these relations $\Delta\epsilon$, σ_{max} and E are respectively the total mechanical strain range, the maximum stress of the cycle and Young’s modulus.

The lifetime equation proposed by Ostergren [16] is:

$$\sigma_T.\Delta\epsilon_p.N_f^{\beta}.\nu^{\beta(k-1)} = C \qquad (4)$$

where ν denotes the frequency, σ_T is the tensile stress and β and k are material constants. A simplest form of this expression is used in our case where no hold time is realised during LCF tests. The modified Ostergren relation is of the following form:

$$\sigma_T.\Delta\epsilon_p.N_f^{\beta}$$

The LCF tests results analysed with the Smith-Topper-Watson and the modified Ostergreen relation respectively are plotted in Figures 7 and 8.

One can observe that the predicted lifetime for the same imposed strain amplitude in LCF tests decreases as a function of increasing temperature using both criteria. The Jaske criterion leads to a smaller dispersion band, due to the variation of Young's modulus with temperature (≈150 GPa at 20°C and ≈80 GPa at 800°C). As a conclusion one can state that the net tensile hysteretic energy permits the smallest scatter of the LCF test results. Unfortunately, the proposed damage indicators do not have a precise physical interpretation and are not intrinsic and therefore not appropriate for lifetime prediction in an anisothermal context.

At this point, in spite of the criticism several remarks can be made. Jaske's criterion represents a direct rough estimation of the dissipated energy per cycle. In an isothermal context, one can easily correlate the amplitude of plastic strain of the Manson–Coffin law with the dissipated energy per cycle. For perfect plasticity, this result is straightforward. For a simple viscoplastic equation, this relation has already been proven by Lemaitre [17].

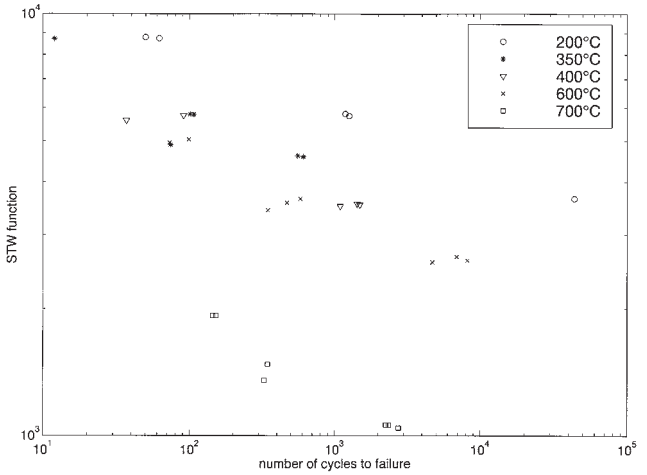

Figure 7 STW function for the SiMo SG cast iron at different temperatures with the test conditions corresponding to Table 2. All values are in J/mm^3.

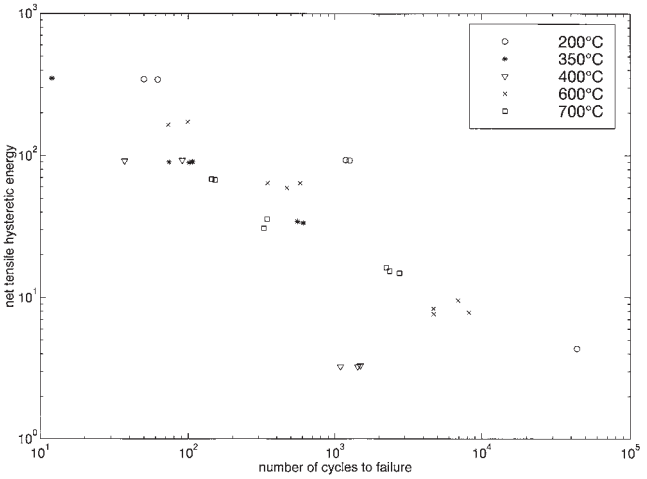

Figure 8 Net tensile hysteretic energy obtained with LCF tests results on SiMo SG cast iron with the test conditions corresponding to Table 2. All values are in J/mm^3.

One can conclude on the importance of the underlying assumptions of Ostergren's criterion:

- only the tensile part of the energy is damaging, as LCF phenomena are driven by growth of crack type defects to a critical size;
- damage does not increase unless a critical threshold stress limit is exceeded. Experience show that this limit can often be neglected;
- damage is dependent on test frequency.

These remarks show that the previous approaches use damage indicators, whose physical interpretation is not too far from a dissipated energy. As a consequence, a precise computation of the dissipated energy could integrate the influence of the preceding phenomena.

In the next section we shall analyse the tests using a energy criterion computed using an adequate elastoviscoplastic constitutive law.

DISCUSSION

The preceding fatigue criteria were completely phenomenological and assumed that the response of a structure to cyclic loading is also cyclic in a strict sense. It is well known [18] that structures and materials exhibit stress hardening or softening to imposed load, depending on a series of factors like the nature of the material, the temperature or the initial state. Starting from this observation, we shall follow the analyses of Skelton [19,20] in order to define a low cycle fatigue criterion for cast iron structures based on dissipated energy.

Cyclic behaviour and accumulated energy

The SiMo SG cast iron presents a short period of hardening at 200, 350, 400 and 600°C (except at ±1% at 600°C) and one of softening at 700°C. Both are followed by a long plateau, as presented for two temperatures in Figure 9.

An interpretation of this behaviour from the point of view of low cycle fatigue has been given by Skelton in [19]. He proposed the identification of three different phases defined respectively by the saturation, tangent and final points, denoted respectively by subscripts : $_{sat}$, $_{tan}$, $_{f}$ (see Figure 10):

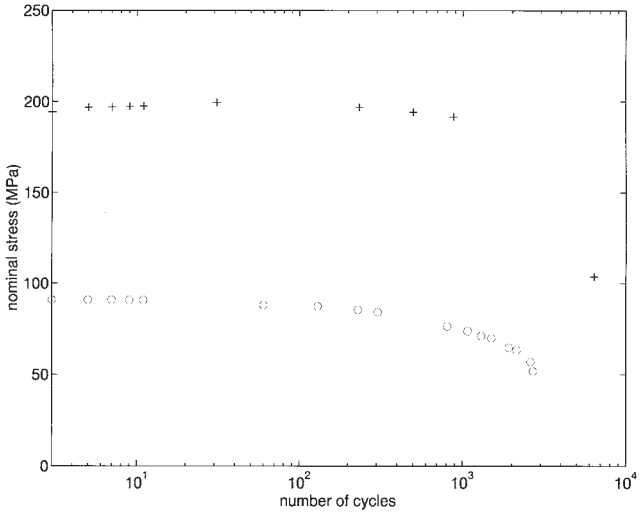

Figure 9 Load versus number of cycles for a LCF test on SiMo SG cast iron at 600°C (+) and 700°C (o) (De = ±0,25%).

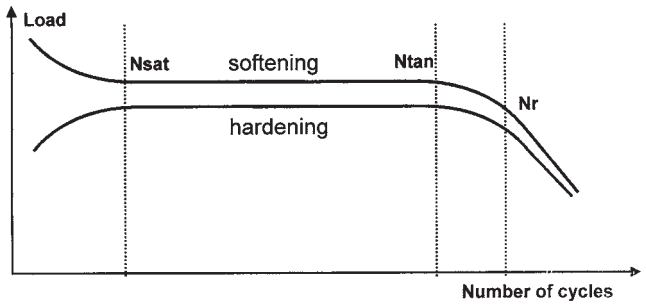

Figure 10 Cyclic behaviour of the material for isothermal LCF tests. Three particular points can be pointed out : N_{sat}, N_{tan} and N_f.

- The hardening/softening phase [0 to N_{sat}] corresponds to the stabilization of the plastic properties of the material. This phase took for cast iron less than 20 cycles at all temperatures.
- The stabilized phase [N_{sat} to N_{tan}] represented by a flat plateau with small property variations. For cast iron this phase is really flat for the tests at 600°C and presents limited softening for the tests at 700°C (see Figure 9).
- a final failure phase [N_{tan} to N_f], where the load drops quickly and failure is inevitable. Conventionally N_f is defined by a 5% or 10% load drop.

Reaching the saturation of the plastic cyclic behaviour implies a stabilized cyclic behaviour of the structure. After Skelton [19] the saturation is reached at N_{sat} for hardening and at N_{tan} for a softening material behaviour. Let us denote by W_{sat} and respectively W_{tan} the accumulated dissipated energies at these points and by W_f the accumulated dissipated energy at N_f.

The measured values of the dissipated energies W_{sat}, W_{tan} and W_f, for cast iron in LCF test at different temperatures, are displayed in Table 5. One can notice that the accumulated energy is very small for the test at temperatures where hardening behavior occurs, *i.e.* 200, 350, 400 and 600°C. This is directly related to the short saturation phase for cast iron. Typically less than 20 cycles passed before N_{sat}, for softening or hardening material behaviour, compared to the several hundreds of cycles in the stabilized phase, N_{tan}–N_{sat}. As W_{sat} and W_{tan} are computed at two different points for hardening or softening behaviour, this also implies that the cumulated energy will have different values. In the case of A316L steel [19,20], Skelton reported similar values of cumulated energy for both types of behaviour. The values are 10–100 times greater in comparison with these obtained for cast iron (see Table 6). This comparison might seem astonishing if one oversees the hundreds of cycles to the saturation point, N_{sat}, observed for steels which easily explain both differences.

It is important to remark, that during stabilized phase, cracks appear in the specimens. For steels their size develops from 0.004 to 0.02 mm at N_{sat} to 0.1–1.5 mm at N_{tan} or N_f as stated by Skelton *et al.* [21]. Even if no similar observations have been made for cast iron, one can assume that the behaviour should be analogous. It is also well accepted that for the softening behaviour one cannot consider N_{tan} as a saturation indicator, due to the development of cracks. Accordingly, it seems natural to consider N_{sat} as an indicator of the saturation of the cyclic material behaviour. This is also justified by the observation that: W_f, the cumulated dissipated energy at N_f is well approximated by: $N_f \times \Delta w_{sat}$, where Δw_{sat} is the dissipated energy per cycle at N_{sat} (see Table 5).

In conclusion, we shall consider that N_{sat} is the stabilized point of the cyclic material behaviour and that Δw_{sat}, the dissipated energy per cycle at saturation is a good candidate to characterize the fatigue loading of the material during the cycles. The stabilized phase is then the part where fatigue damage evolves.

Low cycle fatigue criterion

The conclusion drawn by Skelton *et al.* [21] from observations was a predictive fatigue crack growth criterion as a function of the critical cumulated energy W_{sat} representative of the cyclic behaviour. The crack length observed at N_{sat} for steels in the case of softening or hardening (0.004–0.02 mm) are of the same order of magnitude as the process zone at a crack tip (0.005–0.02 mm). Therefore Skelton *et al.* chose the representative point of the material behaviour for softened materials at the end of rapid softening and not the tangent point where the crack depth is considerably greater than the process zone size. This permits one to express the crack growth rate da/dN as a function of the cumulated energy to saturation W_{sat}, the elastic modulus E and the external load expressed through the stress intensity factor ΔK as follows:

$$\frac{da}{dN} = \frac{\Delta K^2 \cdot (1-\nu)}{2 \cdot \pi \cdot E \cdot W_{sat}}$$

This relation is of great interest as it introduces the stabi-

Table 5 Accumulated energies obtained on SiMo SG cast iron at different temperatures. W_{sat} is taken at N_{sat} for hardened materials and at N_{tan} for softened materials. All values are in J/mm^3 and Δw_{sat} is the dissipated energy per cycle at saturation

Specimen	$\pm\Delta\epsilon$ (%)	W_{sat}	W_{tan}	W_f	$N_f.\Delta w_{sat}$
200°C	0.25	2.8		7.4	6.8
200°C	0.5	1.4		3.4	3.5
200°C	0.5	0.03		3.6	3.6
200°C	1	0.05		0.3	0.6
200°C	1	0.04		0.4	0.7
350°C	0.35	0.07		0.6	0.6
350°C	0.35	0.1		0.6	0.6
350°C	0.5	0.02		0.2	0.2
350°C	0.5	0.05		0.3	0.3
350°C	0.5	0.07		0.3	0.3
350°C	1	0.1		0.1	0.1
400°C	0.25	0.03		0.1	0.2
400°C	0.25	0.02		0.2	0.3
400°C	0.25	0.003		0.2	0.3
400°C	0.5	0.02		0.1	0.1
400°C	0.5	0.09		0.2	0.3
600°C	0.25	0.001		1.8	1.3
600°C	0.25	0.002		1.9	2.5
600°C	0.25	0.001		1.6	1.2
600°C	0.25	0.002		1.1	1.1
600°C	0.5	0.02		0.9	0.9
600°C	0.5	0.007		0.8	1.2
600°C	0.5	0.02		1	1
600°C	1		0.09	0.7	0.7
600°C	1		0.1	0.5	0.5
700°C	0.25		0.5	1	1.1
700°C	0.25		0.6	1.2	1.3
700°C	0.25		0.6	1	1.2
700°C	0.5		0.1	0.4	0.4
700°C	0.5		0.2	0.5	0.5
700°C	1		0.2	0.4	0.4
700°C	1		0.3	0.4	0.4

Table 6 Cumulated energies obtained by Skelton [19,20] on different materials

Values in J/mm^3	W_{sat} mean	W_{tan} mean	W_f mean
A316L	0.69 ± 0.23		1.04 ± 0.18
9Cr1Mo	0.94 ± 0.07	3.20 ± 0.29	
Nimonic 100		0.48 ± 0.20	

lized behaviour of the material as an important parameter for lifetime prediction. It has, however, a drawback as fatigue design cannot be based on a critical crack approach in some industrial applications. For example, in the case of exhaust manifolds, no macroscopic cracks should form during the lifetime and this can be fixed as a design objective. Monitoring crack initiation, propagation, and critical length is a very tedious, if not impossible, task.

However, one can remark that crack growth can be separated into two stages: an initial one where the crack is confined in a small volume and does not influence the macroscopic behaviour of the structure and a final one where the crack length directly influences the load distribution in the structure. The transition point between these two stages is represented by N_f. The design criterion will now require that structures do not enter the final stage during their lifetime.

In conclusion, summarizing all the arguments, one can assume that the stabilized behaviour of the cast iron is well represented by Δw_{sat}, the dissipated energy per cycle at N_{sat}, and that the lifetime is characterized by N_f.

For the LCF tests Δw_{sat} was determined from the experimental strain – stress curve at the N_{sat} point. For TMF tests on specimen or structure Δw was computed using finite elements assuming elastoviscoplastic material behaviour. The energy was computed for a stabilized cycle on the structure. The number of cycles to failure N_f has been ascertained during TMF tests conducted on specimens or exhaust manifolds at the initiation of macroscopic cracks. These results interpreted in terms of predicted versus experimental lifetime are represented in Figure11 and show a good correlation both on specimens and structures.

At this point is interesting to remark in Table 5 that the accumulated energy to failure, computed as $W_f = N_f \times \Delta w_{sat}$ has not a constant value but is a function of the loading level. As Halford has already pointed out, in an exhaustive review of results obtained for steels [22], the accumulated energy to failure, W_f, is a monotonic increasing function of the number of cycles to failure and this is a consequence of the loading dependance of W_f. This is a direct proof that not all dissipated energy is damaging. In order to determine precisely the damaging part of the dissipated energy more studies should be performed. The dissipated energy per cycle did, however, permit the construction of a material objective TMF criterion.

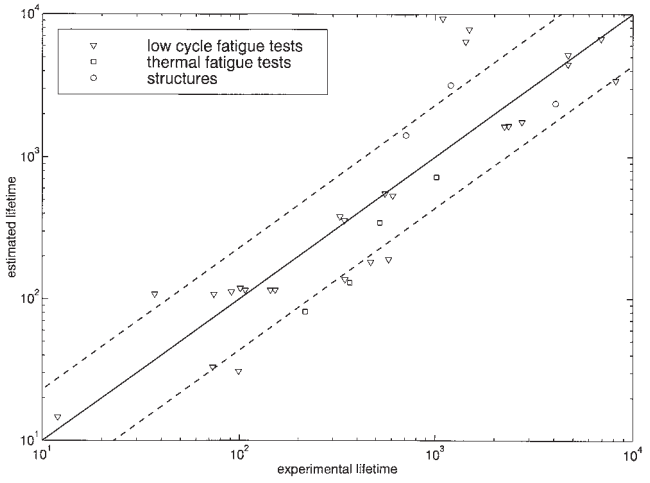

Figure 11 Comparison between experimental and predicted lifetime for LCF and thermal tests and for exhaust manifolds.

CONCLUSION

The purpose of this paper was to define a low cycle thermomechanical fatigue criterion in order to predict failure of engineering structures. Based on LCF test results is has been shown that classical criteria are not sufficient to predict lifetime of complex multiaxial structures. A series of notions like frequency or plastic strain range are not intrinsic from a thermomechanical point of view and, therefore, cannot be employed for characterizing fatigue for complex load paths.

The dissipated energy per cycle does not exhibit these drawbacks and permitted us to explain at the same time isothermal and anisothermal results obtained on cast-iron specimens and structures.

A series of questions related to the dissipated energy remain open:

- how can the damaging part of the dissipated energy be estimated?
- is there a critical, material intrinsic, value characterizing failure or crack initiation energy?
- can one characterize the part of creep and plasticity in the dissipated energy?

ACKNOWLEDGMENTS

The authors would like to thank Ky Dang Van and André Bignonnet for fruitful discussion during this work. This work was funded by PSA (France) and their supported is gratefully acknowledged.

REFERENCES

[1] Chaboche, J.L., Culie, J.P., Gallerneau, F., Nouailhas, D., Pacou, D. and Poirier, D. Thin wall thermal gradient: experimental study, F.E. analysis and fatigue life prediction. *Proceedings of 5th Int. Conf. on Biaxial/Multiaxial Fatigue and Fracture, Cracow '97, Poland*, pp 237–250 (1997).

[2] Dambrine, B. and Mascarell, J.P. Dimensionnement en fatigue et fluage des aubes de turbines. *Aerospatiale*, **1**, 35–45 (1988).

[3] Charkaluk, E., Constantinescu, A., Bignonnet, A. and Dang Van, K. On a failure criterion for thermomechanical multiaxial low cycle fatigue criterion and its industrial application. *Proceedings of LCF4* (Rie, K.T. and Portella, D., eds), *5–11 september 1998, Garmisch-Partenkirschen*, Elsevier, pp. 815–821 (1998).

[4] Feltner, C.E. and Morrow, J.D. Micro-plastic strain hysteresis energy as a criterion for fatigue fracture. *Trans. A.S.M.E.*, 60-MET-2 (1961).

[5] Luong, M.P. and Dang Van, K. Infrared thermographic evaluation of fatigue limit in metals. *27 QIRT Eurotherm Seminar, Paris* (1992).

[6] Solomon, H.D. and Coffin, L.F. Effects of frequency and environment on fatigue crack growth in A286 at 1100F. *Fatigue at elevated temperatures*, ASTM STP 520, pp. 112–122 (1976).

[7] Gell, M. and Leverant, G.R. Mechanisms of high-temperature fatigue. *Fatigue at elevated temperatures*, ASTM STP 520, pp. 37–67 (1976).

[8] Manson, S.S. Behaviour of materials under conditions of thermal stresses. *N.A.C.A.*, TN 2933 (1953).
[9] Coffin, L.F. A study of the effects of cyclic thermal stresses on a ductile metal. Trans. A.S.M.E., **53–A76**, 931–950 (1953).
[10] Bastid, P. Comportement thermomécanique des fontes à graphite sphéroïdal pour collecteurs d'échappement. PhD Dissertation, Ecole Nationale Supérieure des Mines de Paris (1995).
[11] Coffin, L.F. Fatigue at high temperatures. *Fatigue at elevated temperatures*, ASTM STP 520, pp. 5–34 (1973).
[12] Taira, S. Relationship between thermal fatigue and low cycle fatigue at elevated temperature. *Fatigue at elevated temperatures*, ASTM STP 520, pp. 80–101 (1973).
[13] Smith, K.N., Watson, P. and Topper, T.H. A stress-strain function for the fatigue of metals. *J. Mater*., **5**(4), 767–778 (1970).
[14] Jaske, C.E. Thermal-mechanical, low cycle fatigue of AISI 1010 steel. *Thermal fatigue of materials and components*, ASTM STP 612, pp. 171–198 (1976).
[15] Xi, S.X. and Smith, D.J. High temperature fatigue-creep behaviour of single crystal SRR99 Nickel base superalloys: Part II – Fatigue-creep life behaviour. *Fat. Fract. Engng Mat. Struct*., **18**(5), 631–643 (1995).
[16] Ostergren, W.J. A damage function and associated failure equations for predicting hold time and frequency effects in elevated temperatures. *J. Test. Eval.*, **4**(5), 327–339 (1976).
[17] Lemaitre, J. Evaluation of dissipation and damage in metals submitted to dynamic loading. *International Conference on Mechanical Behaviour of Metals* (1970).
[18] Lemaitre, J. and Chaboche, J.L. *Mécanique des matériaux solides*. Dunod, Paris (1985).
[19] Skelton, R.P. Energy criterion for high temperature low cycle fatigue failure. *Mater. Sci. Technol.*, **7**, 427–439 (1991).
[20] Skelton, R.P. Cyclic hardening, softening, and crack growth during high temperature fatigue. *Mater. Sci. Technol.*, **9**, 1001–1008 (1993).
[21] Skelton, R.P., Vilhelmsen, T. and Webster, G.A. Energy criteria and cumulative damage during fatigue crack growth. *Int. J. Fat.*, **20**(9), 641–649 (1998).
[22] Halford, G. R. The energy required for fatigue. *J. Mater*., **1**(1), 3–18 (1966).